Spectral emissivity and radiance temperature plateau of self-supporting Al_2O_3 melt at rapid solidification

Vadim A Petrov, Aleksey Yu Vorobyev

Institute for High Energy Densities, Associated Institute for High Temperatures RAS, 13/19 Izhorskaya, Moscow, 125412, Russia
E-mail: petrov@ihed.ras.ru

Abstract.

The free solidification of a pool of molten Al_2O_3 formed by local heating of solid alumina by concentrated CO_2 laser radiation was investigated. During free rapid cooling from temperature of 2700–2900 K in ambient air and in the course of solidification the high speed pyrometer measured the thermograms of two radiance temperatures at wavelengths of 0.55 and 0.72 μm, the high speed scanning spectrometer measured the intensity of emitted radiation in the wavelength range from 0.5 to 1.3 μm, the infrared spectrometer measured the intensity of radiation of one wavelength, which could be chosen in the range from 2 to 12 μm. Moreover, the pool surface images during solidification were recorded with a CCD camera.
It is obtained that, due to semitransparency of the melt, its emitted radiation depends in the general case on temperature distribution and the optical properties of emitting surface layer. During solidification the spectral emissivity ε_λ in the whole studied spectral region is high and lies in the range from 0.8 to 1. A horizontal plateau of ε_λ and, accordingly, the radiance temperature is observed only in the range of high absorption from 6 to 10 μm. The plateau of ε_λ is absent in the range from 1 to 4 μm. Firstly an increase and then a decrease of ε_λ occur in visible and at the beginning of infrared region.
The received experimental data are analysed by comparison with the results of sufficiently rigorous numerical simulation.

1. Introduction

Refractory oxides of aluminum, zirconium, yttrium, magnesium, and some other elements are semitransparent substances in both the solid and liquid phases. The spectral semitransparent region usually extends from the visible spectrum up to several micrometers. In this region the absorption coefficient may increase from 10^{-3} cm^{-1} to several hundred cm^{-1} as the temperature rises from room temperature to melting. Semitransparent refractory oxides solidify under conditions when the contribution of internal energy transfer by radiation is significant, and often decisive. Because of the high solidification temperature, a high energy flux is removed by radiation from the solidifying melt; under conditions of free cooling in air or vacuum, this fact, along with a low thermal diffusivity of oxide melts, provides for a high cooling rate prior to crystallization.
The processes of rapid crystallization of molten refractory oxides are frequently occurring phenomenon in an actual practice. They take place in the case of plasma spraying of thermal barrier coatings, in the production of fibers and highly dispersed powders, at solidification of droplets in the exhausts of metallized solid propellant rocket motors and in various processes of laser treatment of ceramics. A number of papers have been devoted to the investigation of such processes. The rapid solidification of molten alumina has been considered in most of them, as it is the most studied substance (Nelson et al 1973; Yamada et al 1986; Weber et al 1995a; Plastinin et al 1998; Plastinin et al 2000; Li and Kuribayashi 2004). However, in none of these papers an analysis of the formation of temperature fields upon cooling and

crystallization involved the consideration of the combined radiative-conductive heat transfer (RCHT) within the melt and crystallized substance. This is largely due to the complexity of mathematical formulation of the problem on RCHT in the presence of a phase transition, as well as to the absence of the necessary data on the optical and thermophysical properties of molten refractory oxides and their crystals in the vicinity of the melting point. The temperature plateau observed after undercooling was usually taken to be the radiance (brightness) temperature of solidification T_b. However, a number of questions still wait for answers, namely, the questions of why the pyrometer signal corresponds to T_b of solidification; why the observed plateau sometimes becomes very short, inclined, or even completely disappears; and why the structure of a crystallized layer may be different even for one and the same oxide.

The conventional spectral range of transparency of aluminium oxide, where the absorption coefficient α_λ is less than 10 cm^{-1}, occupies a region approximately from 0.14 to 6.2 μm at room temperature, the long wave edge of this region moves approximately to 4.8 μm and the short wave edge to visible range at the increase of temperature up to 2300 K. The absorption coefficient increases from 0.0014 cm^{-1} to 0.12 cm^{-1} in the range of the least absorption from 2.2 to 2.8 μm (Lingart et al, 1982a). By means of various oblique observations and recently also by direct measurements it is established that α_λ of molten Al_2O_3 in visible and at the beginning of infrared region near melting temperature is more than α_λ of Al_2O_3 single crystal by a factor of tens or even hundreds. However, kinetics and mechanism of change of α_λ at melting and solidification do not understand up to date and it is not clear how the absorption coefficient will be changed at rapid phase transitions. Nevertheless, the melt is semitransparent substance and radiation coming out through the surface of melt at its free cooling and solidification is determined by a temperature distribution and optical properties of emitting surface layer of a certain thickness. However, in many studies it is supposed that in course of solidification the melt is isothermal and its emitted radiation can be characterized by the spectral emissivity, which in one's turn may be determined by measurement of the normal-hemispherical reflectivity (Noguchi and Kozuka 1966, Yamada et al 1986), or can be calculated by using the Fresnel formula, assuming that the melt is optically infinite. The reasoning behind this suggestion is presence of horizontal, exactly, slightly inclined, plateau of the radiance temperature, as a rule at wavelength of 0.65 μm, which is observed at solidification. Chan et al (1983) had shown (apparently, for the first time) that volumetric sources and sink of heat can lead to formation of a two-phase zone consisted of solid and liquid phases of variable concentration. This zone moves in the course of solidification contacting with solidified phase on the one side and with the melt on the other side. However, only the three simplified problems for hypothetical substances with independent of wavelength and temperature optical properties have been considered by Chan et al (1983). Undercooling did not be taken into account, the nature of formation of solid phase nuclei did not be considered, the absorption coefficient was assumed as the same for solid and liquid phases. More realistic simulation of solidification as applicable to aluminium oxide has been done by Petrov et al (1999). The model took into account semitransparency of crystal and melt, dependence of the thermophysical properties on temperature and the optical properties on temperature and wavelength, undercooling before crystallization, and formation of two-phase zone. However, the model did not considered a kinetics of the absorption coefficient change at rapid solidification, it was supposed that at the transition from liquid to solid state the absorption coefficient changes by leaps and bounds. The scattering, which may be in the solidified layer due to porosity and in two-phase zone due to the difference of the refractive index of solid and liquid phases, did not take into account also. So the special experiments need for studying of solidification of molten aluminium oxide at its rapid free cooling in ambient air.

2. Method of measurement and equipment

The first experiments on solidification of molten Al_2O_2 have been carried out by using the set-up for measurement of thermal radiation properties described by Akopov et al (2001). As an example, figure 1 shows the results of two experiments, where the normal-hemispherical reflectivity R_λ at wavelengths of 0.488 and 3.39 μm have been measured. The thickness of melt was about 0.25 mm. The duration of heating by radiation flux of about 1000 W/cm^2 was about 2.2 s. As it may be seen from figure 1, an increase of R_λ begins immediately when the heating is switched off. This is an evidence of absence of the optical infinity in the molten layer even at quasi steady-state conditions when a surface temperature was more than 2900 K. The temperature arrest at solidification took place, however, the horizontal plateau practically was absent and the value of reflectivity at solidification was higher than it must be for optically infinite layer due to reflection of ceramics under the melt.

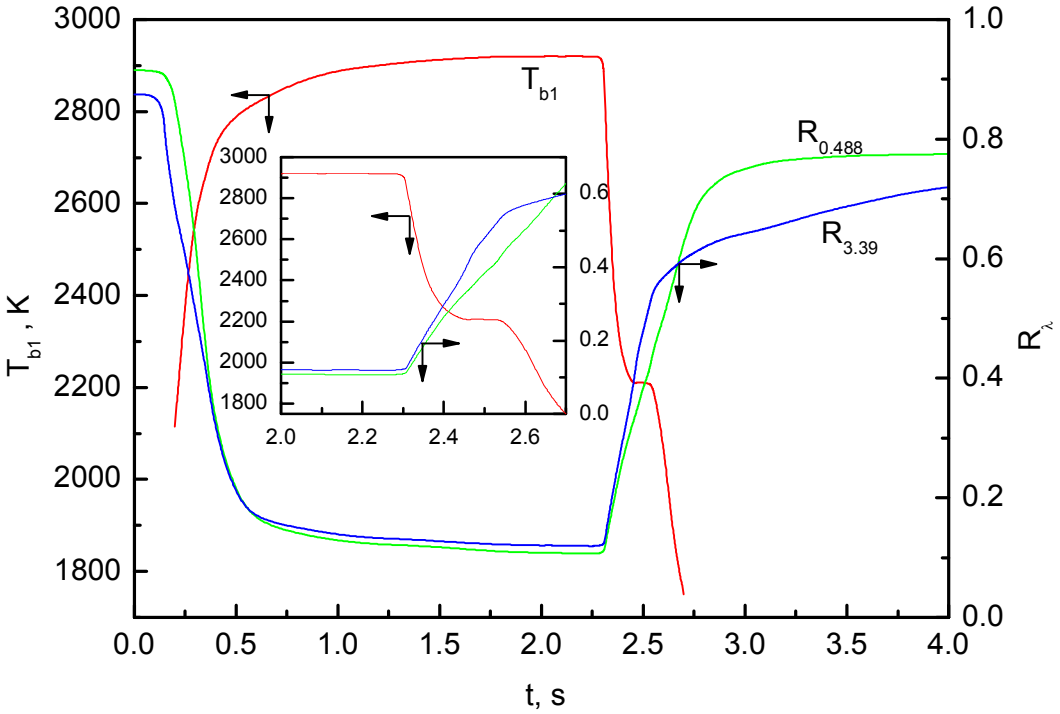

Figure 1. The variation of the radiance temperature T_{b1} at the wavelength of 0.55 μm and the normal-hemispherical reflectivities $R_{0.488}$ and $R_{3.39}$ at wavelengths of 0.488 and 3.39 μm in the process of heating and subsequent cooling.

As at the vertical orientation of the plane sample in the integrating sphere the pool of melt of big thickness did not hold on the sample, the method of measurement and the experimental set-up were changed. Figure 2 is a schematic diagram which shows the experimental arrangement for the main measurements of the emission spectra of molten alumina at rapid solidification. A powder of high pure Al_2O_3 was filled up in the ceramic crucible with an inner diameter of 60 mm and its central part of 25 mm diameter was fused multiple by CO_2 laser radiation and every time after contraction a new portion of fused powder was added. So the dense polycrystalline samples of 4 – 6, sometimes up to 12 mm thick in surrounding of powder were formed. These samples were as an object of investigation. In the course of experiments these samples were heated by CO_2 laser radiation, the radiation flux was about 1000 W/cm^2. Duration of heating was chosen in such a way so as to produce a pool of melt of 3 – 6 mm depth on the surface of polycrystalline sample. At these conditions the temperature of the surface of melt was about 2700 – 2900 K. During heating and subsequent cooling by means of registration of the emitted radiation were measured: the radiance temperatures T_{b1}

and T_{b2} at wavelengths of $\lambda_1 = 0.55$ μm and $\lambda_2 = 0.72$ μm measured by a high speed one range pyrometer, which was calibrated by blackbody radiation; the radiance temperatures in wavelength range from 0.5 to 1.3 μm by a high speed spectrometer, calibrated by blackbody radiation; a signal of a detector of the infrared radiation spectrometer at the wavelength selected beforehand, which could change in the spectral range 2 – 12 μm from one experiment to other. Each of instruments was sighted at the central part of the pool surface of 2 – 3 mm diameter, however, as it may be seen from figure 2, the viewing angles were some different. It might be the reason of small difference between the radiance temperatures, measured by the pyrometer and the scanning spectrometer. The time constant of high speed pyrometer was about 1 ms, the scanning time of the high speed spectrometer was about 15 ms, a pause between spectra was about 85 ms. The CCD camera with the interference filters on wavelengths of 0.48 or 0.63 μm was operated at 25 frames per second. The probing He-Ne laser of 0.6328 μm also was sighted at the centre of the pool surface. A beam diameter was about 3 mm. An incident angle was such as the specularly reflected radiation could not fall into the CCD camera or the scanning spectrometer. The reflected radiation of He-Ne laser can fall into these instruments only in the case of a diffuse reflection.

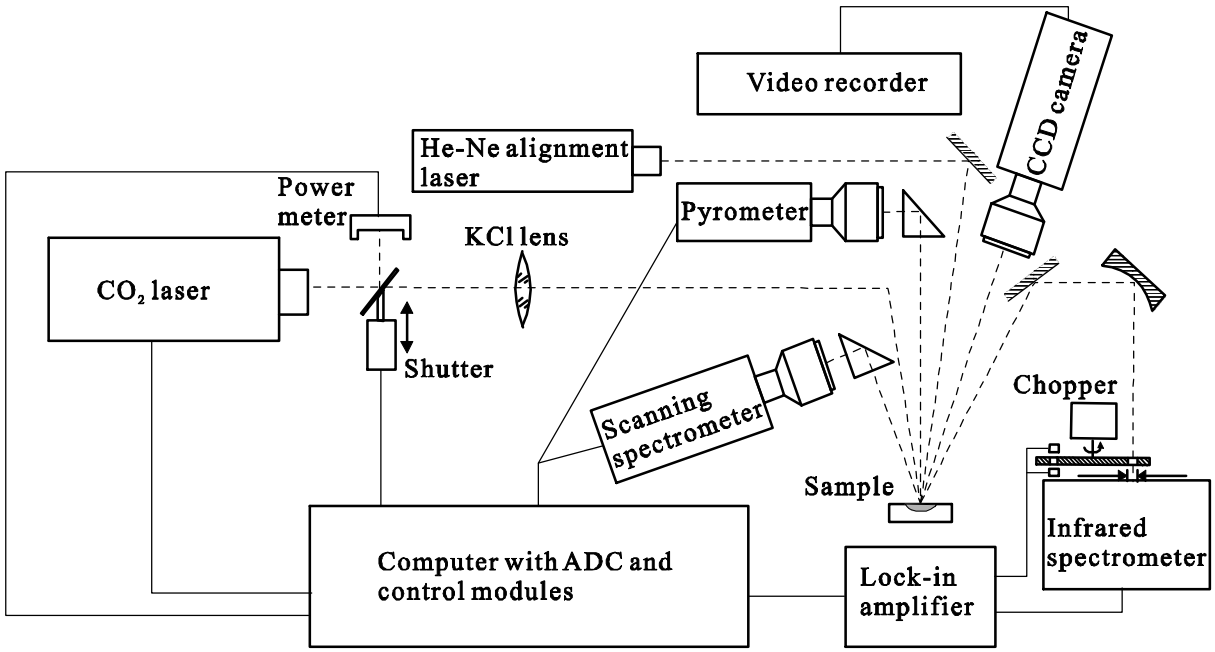

Figure 2. Schematic diagram of the experimental apparatus.

3. Experimental results

The frames, captured by CCD camera, showed that a solidification, as it was expected, started at the periphery of molten pool, where a thickness of melt and its surface temperature were smaller. A solidification process gradually extended to the centre. A central part of 6 mm in diameter begin to solidify simultaneously. It means, that in this part of melt heat transfer is one-dimensional process as the spot sizes of the pyrometer and spectrometer were lesser.

Figure 3 shows, as an example, the results, obtained in one of experiments. The heating time by radiation flux of about 3000 W/cm^2 was 8 minutes, the melt was about 4 mm thick. In the upper part of this figure the time dependence of T_{b1} and T_{b2} and a signal of the infrared spectrometer $U_{\lambda=4\ \mu m}$ at $\lambda = 4.0$ μm are shown, the lower part of figure 3 shows the wavelength dependence of the radiance temperatures, measured by the high speed spectrometer (from 16-th to 42-nd scans, marked by the additional tics on the bottom X axis at the upper part). A long-term horizontal (exactly, slightly inclined) temperature plateau of

solidification was measured by the pyrometer, as soon as the infrared spectrometer at $\lambda = 4.0$ μm such the plateau did not reveal.

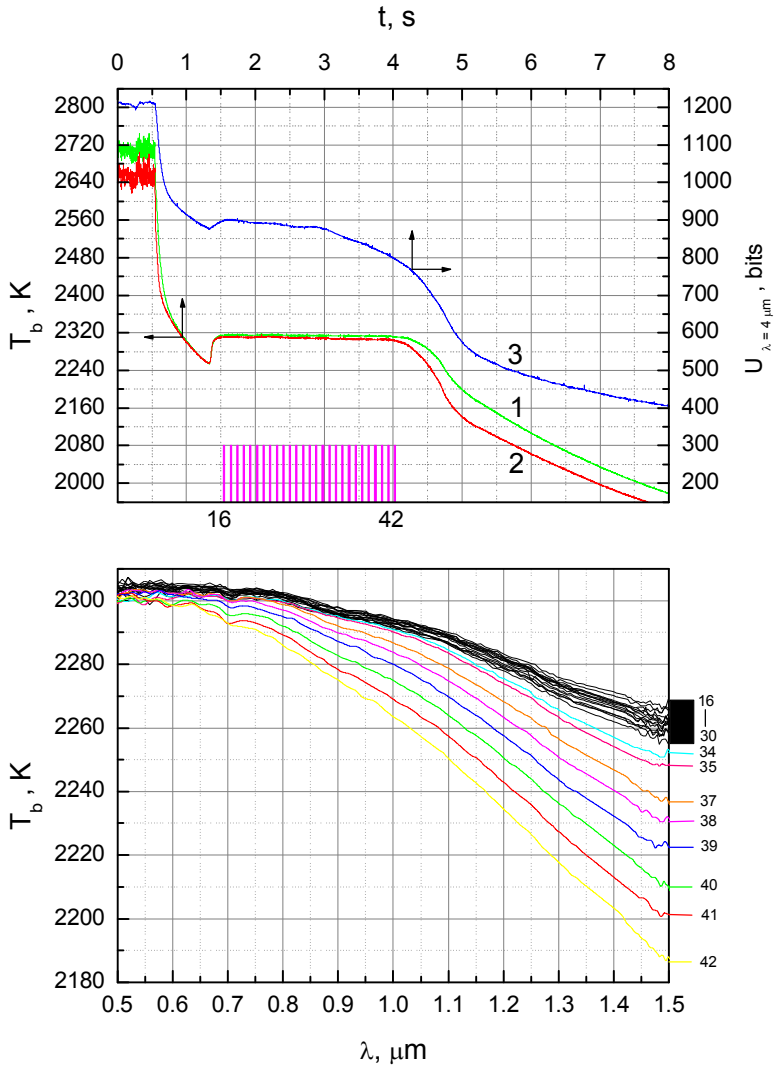

Figure 3. The thermograms and the wavelength dependence of the radiance temperature, obtained in one experiment. Upper graph: 1 – T_{b1}, 2 – T_{b2}, 3 – signal of the infrared spectrometer $U_{\lambda=4\ \mu m}$ at $\lambda = 4.0$ μm; lower graph: the wavelength dependence of the radiance temperatures at the instants, marked at the upper graph.

Figure 4 shows the similar thermograms, obtained in the other experiment. The heating radiation flux was lesser and equal to 1800 W/cm^2, the heating time was about 4 minutes and the thickness of molten layer was about 3 mm. The wavelength of the infrared spectrometer in this experiment was equal to 6 μm. It is seen, that the slightly inclined temperature plateau of solidification is observed both by pyrometer and spectrometer, although the thickness of melt and duration of solidification were lesser. In all, more than 100 experiments were carried out. They differed in the flux of heating radiation, duration of heating, and the installed wavelengths of the infrared spectrometer, which were selected from the series 2, 2.5, 3, 3.5, 4, 5, 6, 7, 8, 9, 10, 11 and 12 μm. Two big groups were selected among the obtained results. In one of them total duration of crystallization was about 4 s, in the other it was about 2.5 s. As it was shown earlier (Petrov et al, 1999), at solidification a considerable part of cooling melt is the isothermal two phase zone, which temperature is equal to the melting (solidification)

temperature. At that the temperature of surface is very close to the solidification temperature even if a thin crust is formed on the surface. So the radiation, emitted by solidified melt, may be characterized by the emissivity ε_λ, assuming, as usual, that

$$\varepsilon_\lambda = I_\lambda(T_m) / I_\lambda^0(T_m) \qquad (1)$$

where $I_\lambda(T_m)$ - the intensity of radiation, emitted by melt, $I_\lambda^0(T_m)$ - the intensity of radiation, emitted by blackbody at temperature of solidification (melting) T_m.

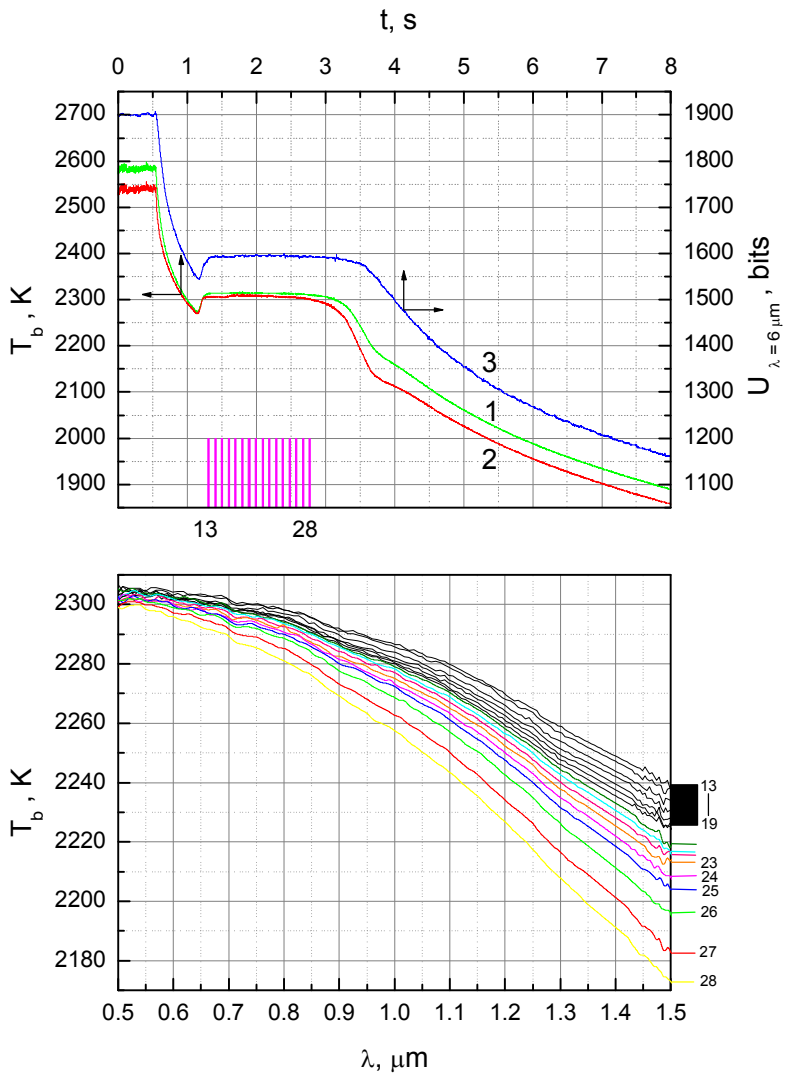

Figure 4. The thermograms and the wavelength dependence of the effective temperature, obtained in one experiment. Upper graph: 1 – T_{b1}, 2 – T_{b2}, 3 – signal of the infrared spectrometer $U_{\lambda=6\ \mu m}$ at $\lambda = 6.0$ μm; lower graph: the wavelength dependence of the radiance temperature at the instants, marked at the upper graph.

As the pyrometer and the high speed scanning spectrometer were calibrated using the blackbody model, the following way of calculation of ε_λ was used:

1. The values of the radiance temperatures at the pyrometer wavelengths of 0.55 and 0.72 μm were averaged on the initial section of 0.1 – 0.2 s of the solidification plateau after undercooling.
2. As the solidified melt at this stage was optically infinite for the pyrometer wavelengths, the true solidification temperature was calculated, using measured radiance temperatures and the normal reflectivity, calculated by using Fresnel formula

and the value of the refractive index of molten Al_2O_3 $n = 1.744$, obtained by Krishnan et al (1991). The specular character of reflection of the melt at the initial section of solidification was established by the CCD camera and scanning spectrometer. The CCD camera recorded an appearance of a bright spot on the surface due to a diffuse component of probing laser reflection only after 160 – 200 ms from the beginning of solidification. Approximately at this time the peak of spectrometer signal at wavelength of 0.63 μm appeared. Then the value of this spectrometer peak gradually increased. The frames of CCD camera showed that the bright spot on the surface was not positioned at the same place, but shifted on the surface. Only at the middle of plateau its position became fixed. The mean value of the true solidification temperature for all experiments, based on the measurement by the pyrometer and calculated as in was mentioned above, was equal to $T_m = 2329$ K, that is very close to the recommended value 2327 K (Chase et al, 1985).

It may be noted, that the instant of finishing of solidification on the base of thermograms may be determined very approximate. As it may be seen from the comparison of figures 3 and 4, very small decrease of the radiance temperatures for the wavelengths of 0.55 and 0.72 μm is observed at the initial part of the solidification plateau. In the first case it takes about 2.5 s, in the second case – about 1.75 s. After this the decrease of T_{b1} and T_{b2} accelerates up to appearance of fracture when the rate of decrease becomes lesser. A similar character of change of the radiance temperature at $\lambda = 4$ μm can be seen in figure 3, however, a stage of small decrease of radiance temperature is shorter than for the wavelengths of the pyrometer. At wavelength of 6 μm the slightly inclined plateau of solidification is more prolonged than at the wavelengths of the pyrometer (see figure 4), and at the following stage of an acceleration of T_b decrease the fracture of dependence $T_b(t)$ is absent. It was obtained that the fracture is observed in the spectral range of melt transparency from 0.5 to 4 μm. Its appearance causes by big decrease of the absorption coefficient at solidification. As the wavelength increases further in the infrared region, the absorption coefficient as solid as molten Al_2O_3 increases and a registered radiation determines by an emission of more and more thin sub-surface layer. The time of finishing of solidification may be assumed as an instant, corresponding to an acceleration of decrease of the temperature at wavelength of 10 μm at the end of solidification plateau. At this wavelength the absorption coefficient of solid Al_2O_3 is near maximum and the refractive index is near 1 (Lingart et al, 1982b). So the radiance temperature at this wavelength is practically the true temperature of surface.

As the infrared spectrometer was not calibrated on the blackbody radiation, and only the signal of this spectrometer during cooling and solidification of melt was measured, the value of ε_λ in the spectral range from 2 to 12 μm was calculated using the true temperature of solidification T_m, obtained as it was mentioned above and assumed as constant for the whole plateau, and a value of the radiance temperature. The latter was calculated for the whole plateau of solidification, using an assumption that at the initial stage of solidification $\varepsilon_\lambda = 1 - R_\lambda$ and using the known data on the refractive index n_λ. As the values of n_λ of molten Al_2O_3 in the spectral range of 2 – 12 μm are unknown, the recommended data (Lingart et al, 1982a, b) for the single crystal of Al_2O_3 were used. In the spectral range from 2 to 6 μm these data were taken for temperature of 2293 K, which is close to the melting temperature, and in the range from 7 to 12 μm – at temperature 1773 K, which is the highest for the published data in this range.

The obtained results for time dependence of ε_λ at different wavelengths at the solidification plateau for two groups of experiments mentioned above are shown in figures 5 and 6. In these figures also the time dependence of the radiance temperature for two wavelengths of the pyrometer is shown. In this case the radiance temperatures were corrected on the surface

reflection using the Fresnel formula. Each curve of $\varepsilon_\lambda(t)$ in the spectral range 2 – 11 μm, shown in figures 5 and 6, is the result of separate experiment. In the range of measurement by scanning spectrometer from 0.5 to 1.3 μm the shown dependences $\varepsilon_\lambda(t)$ for different wavelengths are the results of the single experiment, however, these results are typical for the other experiments of the group with the same duration of solidification.

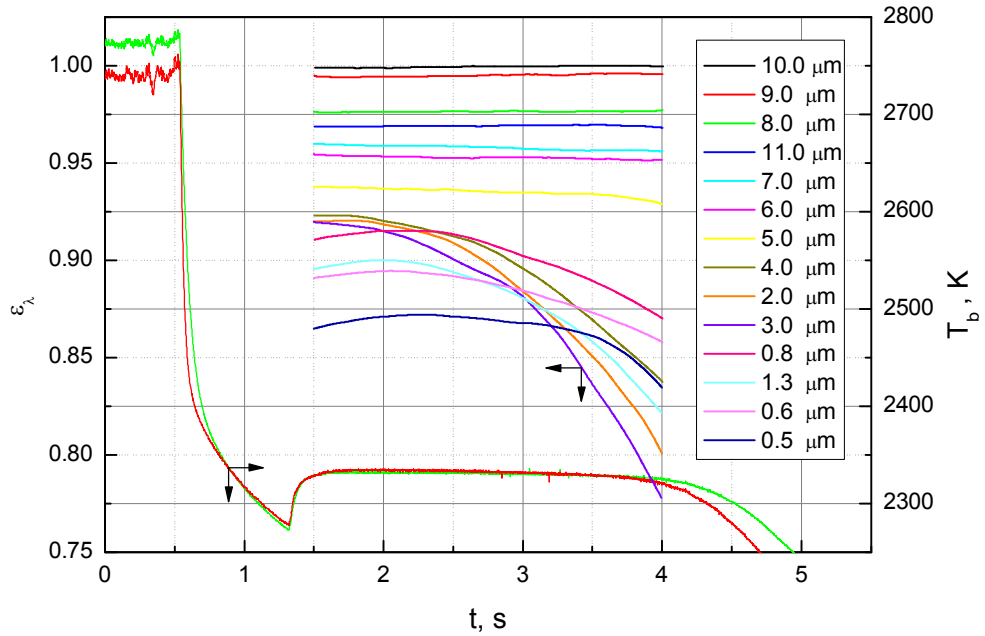

Figure 5. The spectral normal emissivity at different wavelengths during solidification at total duration of crystallization about 4 s.

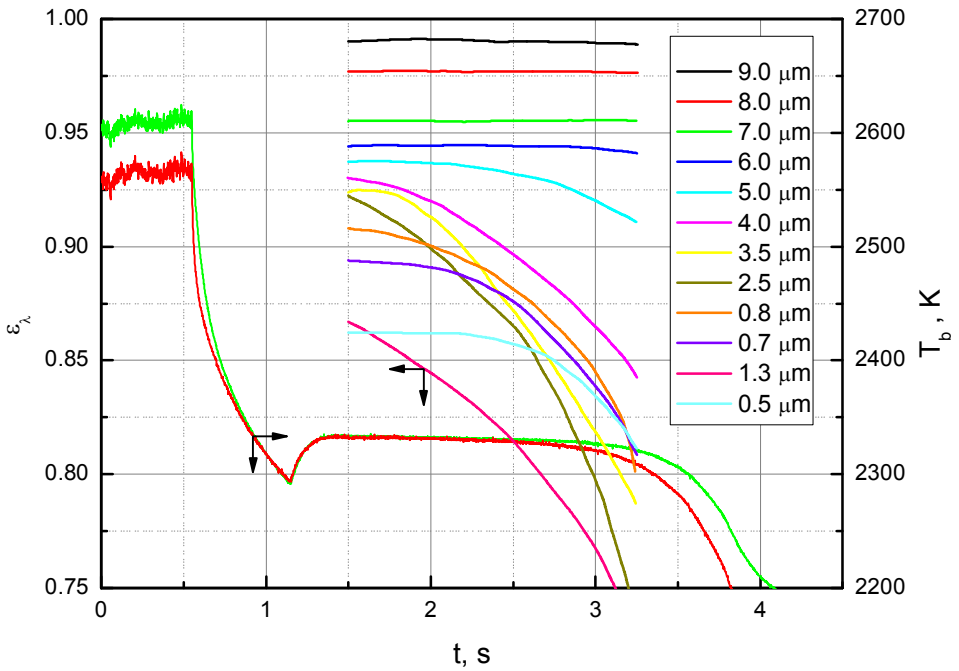

Figure 6. The spectral normal emissivity at different wavelengths during solidification at total duration of crystallization about 2.5 s.

Along with a detailed study of two group of experiments with total duration of solidification about 4 and 2.5 seconds, some measurements with the thicker melt and, accordingly, longer solidification were carried out. Figure 7 shows the results of one such experiment with

duration of solidification about 5.5 s. It may be seen that there are some differences from the results for two groups demonstrated above. In this experiment at the initial stage of solidification plateau in the range 0.7 – 1.3 μm ε_λ does not depend on time and there is a little or no dependence on wavelength. The values of ε_λ are somewhat lesser only at wavelengths of 0.6 and 0.5 μm. At the initial stage of plateau an increase of ε_λ is absent even at these short wavelengths.

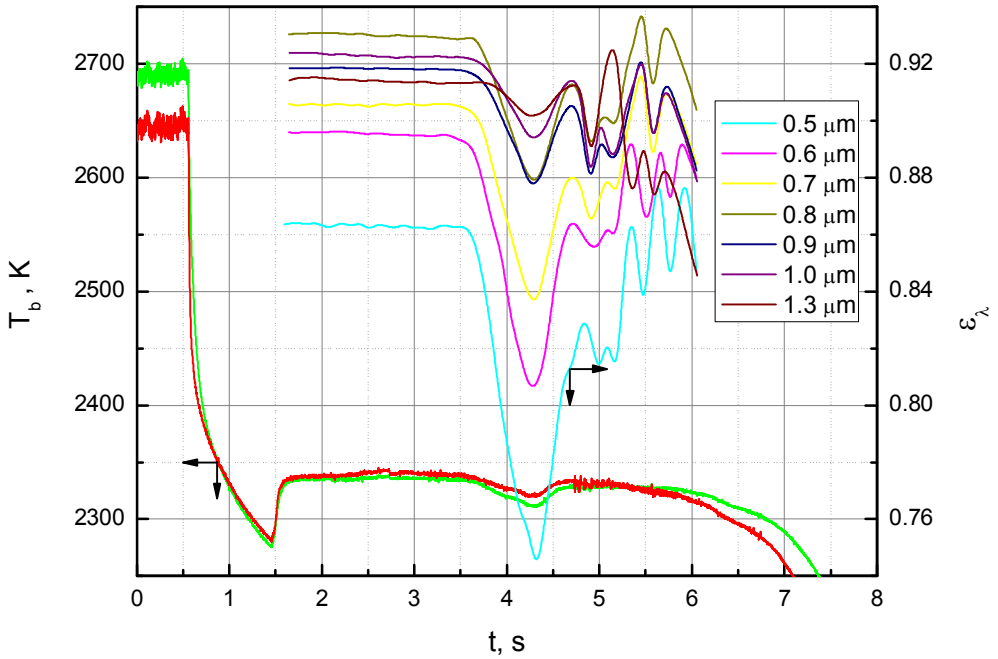

Figure 7. The thermograms and the spectral normal emissivity at different wavelengths at total duration of crystallization about 5.5 s.

A non-monotone change of the emissivity in the spectral range of scanning spectrometer and the radiance temperatures, measured by the pyrometer are observed in the latter half of the plateau. Beginning at some instant the signals of both channels of pyrometer and the spectrometer in the whole spectral range decrease. As it was registered by CCD camera, before decreasing of these signals the bright spot of reflected He-Ne laser radiation, which was seen due to the diffuse component of reflectivity, disappeared. The decrease of signals is limited and an increase begins soon. The signals restore almost up to values that were observed before their decrease. Then the signals reveal some oscillations, lesser by long and amplitude. This character of change of signals was reproduced in different experiments, where the duration of solidification was very long.

4. Analysis of experimental results

The available data on the spectral emissivity of Al_2O_3 during solidification are absent in literature. In the most similar study of Brun et al (2003) the spectral emissivity is measured in the broad wavelength range, but the temperature was below and above the melting point. The process of solidification was not studied. So as the comparison of our results with the literature data is impossible, the analysis can be carried out in the frame of obtained experimental results and previous results on numerical simulation of combined radiation and conduction heat transfer at heating and solidification (Petrov et al, 1999).

At the first let us consider an inferable character of crystallization. As the molten Al_2O_3 at high temperatures has a big absorption coefficient and the greatest temperature in quasi steady-state conditions is at the surface, at the beginning of cooling after blocking of CO_2 laser radiation a maximum cooling rate takes place at the sub-surface layer and two-phase

zone appears near the surface (Petrov et al 1999). Figure 8 shows the microstructure of the cross fracture of the solidified layer. The surface layer about 450 μm thick consisted of two sub-layers, namely, the upper dendritic sub-layer approximately 250 μm thick (the dendrite axes extending in the direction perpendicular to the surface) and the lower sub-layer consisting of particles which are more isometric. The surface layer was followed by a zone of large columnar crystals. Voids and microcracks were observed in both sub-layers, which might cause scattering. It may be supposed that the nuclei of crystallization were formed at the surface, as here the undercooling appeared earlier. Very small isolated dendrites grew from the nuclei deep into undercooled melt in the direction perpendicular to the surface and at that they were surrounded by the melt, so the reflection of the surface after the beginning of solidification continued to be specular. So a two-phase zone appeared near the surface. Outside the two-phase zone if to move away from its boundary the temperature was more and more, reached the maximum and then decreased. At the far (internal) boundary of the melt temperature was equal to the melting (solidification) temperature. Of course, the solidification took place at this boundary also, however, due to poor heat rejection to alumina powder, it was very slow. Hence, the melt in the course of solidification near the both boundaries had the temperature of melting, and inside the melt temperature was higher. In the course of solidification the maximum of temperature gradually decreased. After 160 – 180 ms from the beginning of solidification the dendrites outgrew up to appreciable size and a crust was formed at the surface. However, this crust was not continuous and plate due to a big increase of density at solidification. Thus the diffuse component of reflection appeared.

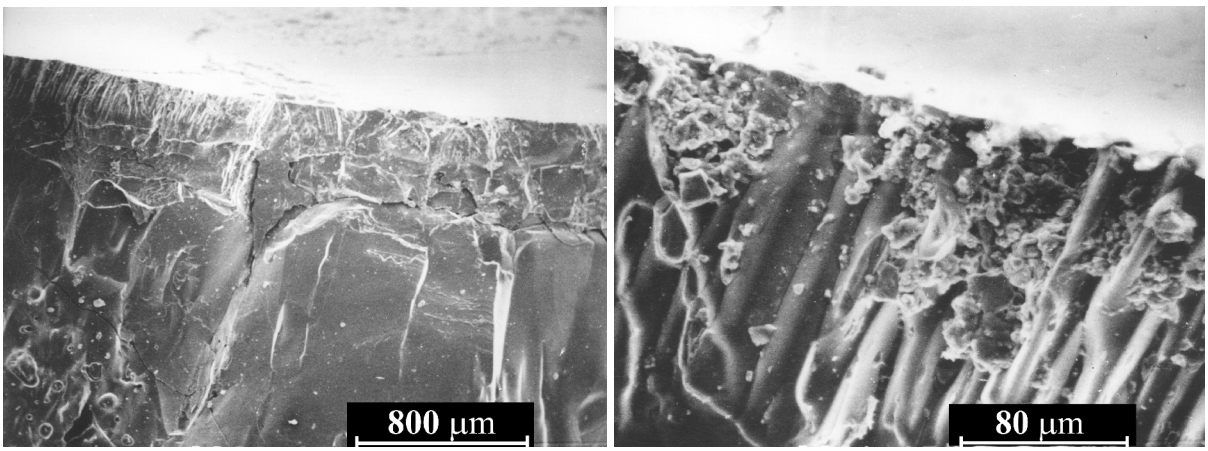

a b

Figure 8. The structure of cross fracture of crystallized surface layer: a – general view, b – sub-surface layer.

Considering jointly figures 5 and 6, some general feature and differences can be noted. At first it can be marked that during solidification ε_λ is very high. It is more than 0.9 in the wavelength range from 5 to 11 μm. At shorter wavelength it is not less than 0.7. This is evidence of the high absorption coefficient of molten Al_2O_3. In the spectral range of high absorption at wavelength more than 6 μm, where even in solid Al_2O_3 near melting temperature the absorption coefficient is more 60 cm^{-1} (Lingart et al 1982a), the values of ε_λ are the most high and do not depend on the thickness of melt. So it can be assumed that temperature in sub-surface emitting layer at the solidification plateau is constant practically and the same for the samples with the melt of different thickness. So the wavelength dependence of the emissivity (reflectivity) in this spectral range causes by the change of the refractive index, which decreases monotonely from 1.56 to 1 as the wavelength changes from 6 to 10.5 μm.

At wavelengths shorter than 6 μm in IR region the decrease of ε_λ is observed as the solidification approaches to the end. The decrease is the more, the shorter is wavelength, i.e. the absorption coefficient is lesser.

At the wavelength of 5 μm the absorption coefficient of solid Al_2O_3 near the melting point is about 14 cm^{-1}. It means that at the thickness of several mm the solidified melt is optically infinite, and the decrease of ε_λ at solidification can not be explained by the decrease of the absorption coefficient. After completion of solidification ε_λ at 5 μm will be determined by emitted radiation of the layer with thickness about 1.5 mm. The decrease of temperature in this layer, when solidification moves deep into the melt, is absent, as the measurements at wavelengths of 7 μm and more show, that the temperature of the sub-surface layer in the course of solidification does not decrease.

Supposed reason of decrease of ε_λ at the wavelength of 5 μm may be the scattering of radiation by voids and pores in the emitting layer. There are two reason of formation of voids and pores. The first is caused by an increase of the density of Al_2O_3 at solidification almost on 30% (Maurakh and Mitin 1979). The second may be caused by release of gases dissolved in the melt (Bagdasarov 1974). As it can be seen in figure 8, in solidified melt there are as the voids of various arbitrary shape as the spheroidal voids. Both may be the reason of scattering. When the absorption coefficient is big, the scattering influences on the emissivity little, but when the absorption coefficient is small, its role can be considerable.

The decrease of ε_λ in visible and at the beginning of IR region (0.5 – 1.3 μm) during solidification is determined first of all by the low absorption coefficient of solid phase, which changes from 0.4 to 0.2 cm^{-1} in this range. This means that the solidified melt of several mm thick is not optically infinite and in the course of solidification the optical infinity vanishes and the transmission appears. Little by little the more deep layers, which were not molten and have lesser temperature, begin to make their contribution into the emitted radiation. In this spectral range there is a difference between results for the melt of different thickness. As it may be seen from figures 5 and 6, the emissivity of the sample with the thicker molten layer at the beginning of solidification increases, whereas ε_λ of the sample with thinner melt decreases during solidification from its start. The reason may be different temperature distribution in the melt before the beginning of solidification. Before solidification the maximum of temperature in the middle part of thicker melt is pronounced. As the crystallization is accompanied by discontinuous decrease of the absorption coefficient in this spectral range from 20 – 40 cm^{-1} (Weber et al 1995b) to 0.4 – 0.2 cm^{-1}, the sub-surface solidified layer quickly becomes practically transparent and the radiation of more deep layers with higher temperature begins to come out it. At cooling of the samples with thinner molten layer, the maximum of temperature in the middle of the melt, when the temperature of the surface approaches the solidification temperature, is much less or absent at all. So increase of ε_λ during solidification is not observed.

Analysis of data on changing of the emissivity in the course of solidification reveals that in molten Al_2O_3 near the melting temperature the minimum of the absorption coefficient takes place in the region 1.3 – 3.0 μm. The flat part of temperature plateau in this range is absent at all studied thickness of the melt.

As it was mentioned above, the duration of the solidification plateau depends on the thickness of melt and it is different for various wavelengths at the same thickness of melt. Figure 9 shows the comparison of results for the radiance temperatures at some wavelengths, obtained in the course of cooling and solidification for the melt of 3 mm thick. The starts of cooling reduced to the same instant. It is seen that among shown results the almost horizontal plateau is observed at wavelengths of 0.55, 5.0 and 9.0 μm. The radiance temperatures at these wavelengths do not have a big change of slope of $T_b(t)$ dependence after the end of

solidification. But at two other wavelengths 2 and 3 μm this change is very big and take place in the stretch of time 4.5 – 6 s, when the radiance temperatures about 1930 K and 1800 K correspondingly. The reason may be the big decrease of the absorption coefficient due to the change of coordination surroundings of Al atoms and realignment of electronic structure at the liquid – solid transition (Landron et al, 2001a, b).

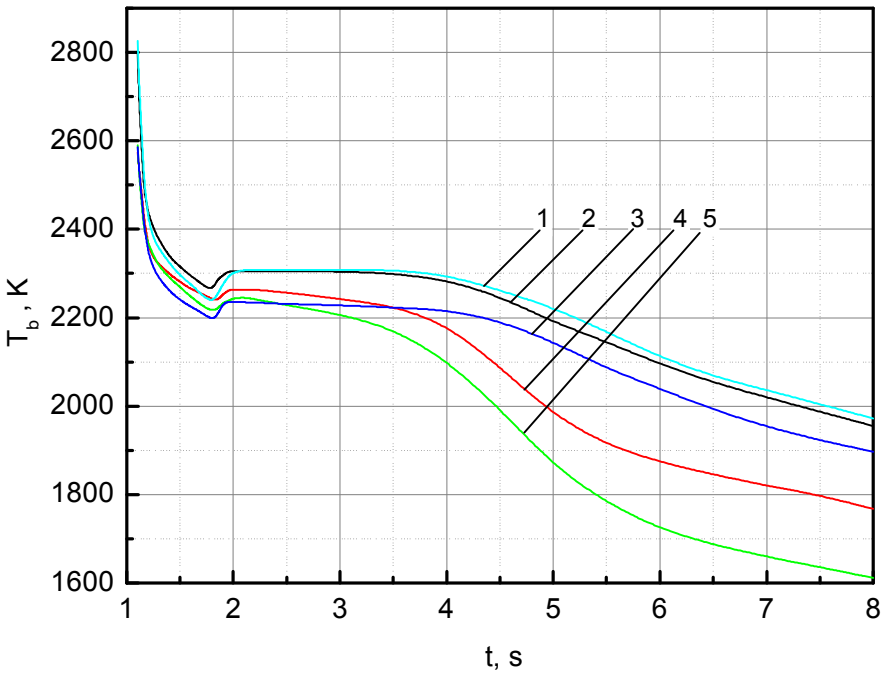

Figure 9. Radiance temperatures at cooling and solidification of samples with molten layer of 3 mm thick: 1 – 9 μm, 2 – 0.55 μm, 3 – 5 μm, 4 – 2 μm, 5 – 3 μm.

5. Conclusion

The experimental results obtained show that due to semitransparency of the melt its emitted radiation in the course of solidification depends in the general case on temperature distribution and the optical properties of emitting surface layer. A lengthy horizontal plateau of ε_λ and, accordingly, the radiance temperature is observed only in the range of high absorption from 6 to 10 μm. A gently inclined plateau of ε_λ at 5 μm takes place only at the first part of the solidification process. The plateau of ε_λ is absent in the range from 1 to 4 μm. Firstly an increase and then a decrease of ε_λ occur in visible and at the beginning of infrared region. The horizontal section of the plateau of ε_λ may be obtained in this region by increasing of melt thickness. As a whole, there is quite good agreement between calculated data, obtained by use of the model taking into account the formation of two-phase zone, and the experimental results. However, it is shown that used in the mathematical model an abrupt stepwise decrease of the absorption coefficient at solidification does not correspond well to the obtained experimental data.

Acknowledgement

This work was supported by the Russian Foundation for Basic Research, project № 05-02-16290.

References

Akopov F A, Val'yano G E, Vorob'ev A Yu, Mineev V N, Petrov V A, Chernyshev A P, Chernyshev G P, 2001 *High Temperature* **39** 244-254

Bagdasarov Kh S, 1974 in *Rubin i Sapfire* (Ruby and Sapphire) Ed. L M Belyaev (Moscow: Nauka) pp. 20-23

Brun J F, De Sousa Meneses D, Echegut P, 2003 *CD-ROM Proceedings of the Fifteenth Symposium on Thermophysical Properties,* Boulder, Colorado, USA

Chase R W, Jr, Davies C A, Downey G R, Frurip D J, McDonald R A, Syverud A H, 1985 *JANAF Thermochemical Tables, J. Phys. Chem. Ref. Data* **14, Suppl. 1** 156

Chan S H, Cho D H, Kocamustafaogullary G, 1983 *Int. J. Heat Mass Transfer* **26** 621-633

Krishnan S, Weber J K R, Schiffman R A, Nordine P C, Reed R A, 1991 *J. Amer. Ceram. Soc.* **74** 881-883

Landron C, Hennet L, Jenkins T E, Greaves G N, Coutures J P, Soper A K, 2001 *Phys. Rev. Letter* **86** 4839-4842

Landron C, Soper A K, Jenkins T E, Greaves G N, Hennet L, Coutures J P, 2001 *Journ. Non-Cryst. Solids* **293-295** 453-457

Li M, Kuribayashi K, 2004 *Journ. Appl. Phys.* **95** 2342-2347

Lingart Yu K, Petrov V A, Tikhonova N A, 1982a *Teplofisika vysokikh temperatur* **20** 872-880

Lingart Yu K, Petrov V A, Tikhonova N A, 1982b *Teplofisika vysokikh temperatur* **20** 1085-1092

Maurakh M A, Mitin B S, 1979 *Zhidkie Tugoplavkie Okisly* (Liquid Refractory Oxides) (Moscow: Metallurgiya) 288 pp

Nelson L S, Richardson N L, Keil K, Skaggs S R, 1973 *High Temp. Sci*. **5** 138-154

Noguchi T, Kozuka T, 1966 *Solar Energy* **10** 125-131

Petrov V A, Titov V E, Vorobyev A Yu, 1999 *High Temp. – High Press*. **31** 267-274

Plastinin Yu A, Sipatchev H Ph, Karabadzhak G F, Khmelinin B A, Szhenov E Yu, Khlebnikov A G, Shiskin Yu N, 1998 *AIAA Paper* N 98-0862

Plastinin Yu A, Sipatchev H Ph, Karabadzhak G F, Khmelinin B A, Szhenov E Yu, Khlebnikov A G, Shiskin Yu N, 2000 *AIAA Paper* N 2000-0735

Weber J K R, Anderson C D, Merkley D R, Nordine P C, 1995a *J. Am. Ceram. Soc*. **78** 577-582

Weber J K R, Krishnan S, Anderson C D, Merkley D R, Nordine P C, 1995b *J. Am. Ceram. Soc*. **78** 583-587

Yamada T, Yoshimura M, Somiya S, 1986 *High Temp. – High Press*. **18** 377-388